

Enhanced hard X-ray emission from femtosecond laser irradiated microdroplets

M. Anand, M. Krishnamurthy*, A. S. Sandhu and G. Ravindra Kumar
Tata Institute of Fundamental Research, 1 Homi Bhabha Road, Mumbai 400 005, India.
(Dated: December 2, 2024)

We demonstrate that 15 μm methanol microdroplets efficiently absorb intense femtosecond laser pulses, resulting in the production of very hot electrons even at moderate intensities. A hot electron temperature of 36 keV is measured from the droplets at $8 \times 10^{14} \text{ W cm}^{-2}$; three times higher intensity is needed to obtain similar hot electron temperature from solid plasmas. The hard X-ray yield from droplet plasmas is $\simeq 250$ times more than that obtained from solid plasmas under similar conditions. The higher yields and temperatures in microdroplets are explained in terms of the differences in scattering of light from droplets and solid surfaces. Mie scattering calculations of the intensity distribution inside the droplet indicate an order of magnitude enhancement of the incident intensity inside the microdroplet.

PACS numbers: 79.20.Ds, 52.25.Os, 52.38.2r, 52.50.Jm

The physics of laser-plasma interactions has undergone a revolution in recent times. Technological advances in lasers have opened the possibility of delivering joules of energy in femtosecond time scales to achieve intensities upto $10^{21} \text{ W cm}^{-2}$ [1]. The non-perturbative physics of laser-matter interactions at these extreme intensities has brought forth many new concepts and applications [2]. Novel schemes of pulsed neutron generation [3] and nuclear reactions [4] have been demonstrated. Table top accelerators [5] and synchrotrons [6] are no longer considered as mere predictions. Hot, dense laser produced plasmas are a promising source of radiation, both in EUV and x-ray regimes; developing efficient sources of such radiation is one of the key problems. One of the main aims of laser-plasma interaction studies is to develop strategies to efficiently couple laser energy into matter to enhance high energy ion, electron and photon emission. To this end, introduction of novel targets as the recipient of the laser energy has been very fruitful. Metallic nanoparticle-coated solids [7] and 'velvet' targets [8] have yielded enhanced x-ray emission in the moderate to very hard x-ray regime. Another example are clusters, which are nanoparticles with solid-like local density, which have been shown to absorb 90% of the incident laser energy [9]. Particle acceleration upto an MeV has been achieved in such systems at intensities of $10^{16} \text{ W cm}^{-2}$. Efficient nuclear fusion has been demonstrated with the use of D_2 clusters.

There are, however some disadvantages in the use of gaseous cluster systems, one of which is that the kind of atomic or molecular species that can be used for the production of large clusters is very limited. For example, there is no simple way to generate large clusters with high-Z atoms like Pt. The use of liquid droplets is a promising alternative. Droplet targets are debris-less and

couple the advantage of size confinement, along with the relative ease with which a droplet may be used to introduce any atomic/molecular system of interest. Droplet targets have found application in EUV Lithography and X-ray microscopy [10, 11]. The emphasis on droplet plasma studies has so far been mostly towards measuring and optimizing the EUV radiation at 13 nm which is the chosen radiation for lithographic purposes, though there have been some initial studies towards measuring hard x-ray radiation [12, 13, 14]. The study of hard X-ray emission from droplets is even more interesting, given that there is very little hard X-ray emission from clusters of energy above 5 keV [15].

In this paper, we present measurements of hard x-ray emission, in the range 50-200 keV, from 15 μm methanol droplets irradiated with 100 fs laser pulses with intensities up to $3 \times 10^{15} \text{ W cm}^{-2}$. We also measure hard X-ray emission from a solid plastic target under similar conditions for comparison. Even at these moderate intensities, hot electron temperature as large as 36 keV has been obtained in the case of droplet targets. Experiments with solid plastic targets, indicate similar temperatures only at three times higher intensities. The X-ray yield from the droplet plasma is at least two orders of magnitude larger compared to that obtained from solids at similar intensities. At intensities less than $3 \times 10^{15} \text{ W cm}^{-2}$, where we measure copious yield of hard x-rays from droplets, we do not observe any measurable hard x-ray emission in the range of 50-200 keV from solid targets. The efficient hard X-ray emission in droplets has been explained using simple physical explanation and appropriate numerical calculation based on the Mie scattering formalism.

The microdroplet targets are generated by forcing methanol through a 10 μm capillary, which is modulated at 1 MHz frequency using a piezo-crystal. The uniformly sized droplets were characterized by direct imaging of the droplet, and also by observing morphological dependent resonances (MDR)[16]. In direct imaging, we illuminate

*email:mkrisim@tifr.res.in

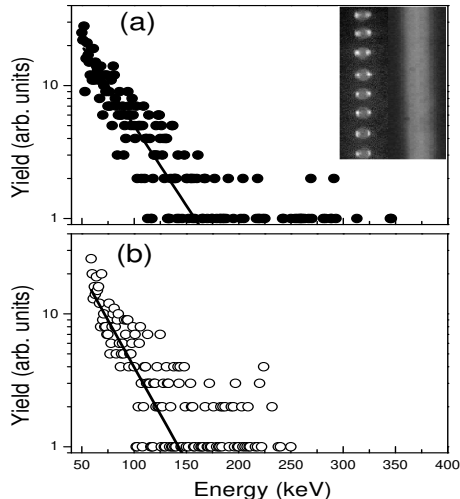


FIG. 1: a). X-ray emission spectra obtained when $15\mu\text{m}$ methanol droplet are irradiated at $8\times 10^{14}\text{ W cm}^{-2}$. The solid line shows the least square fit to the data assuming a Maxwellian distribution for the electrons of 37 keV temperature. The inset shows an image of the droplet stream along with the image of a precision $20\mu\text{m}$ slit used for determining the size of the droplet. b) X-ray emission spectra obtained when a solid plastic target is irradiated with similar laser pulses at an intensities of $2.5\times 10^{15}\text{ W cm}^{-2}$ at 45° to the normal using P-polarized light. The solid line shows the least square fit to the data assuming a Maxwellian distribution for electron of 31keV temperature.

the drops with a picosecond strobe light and capture an image using a CCD camera fitted with a $20\times$ microscopic objective. The inset in figure 1(a) shows the droplets along with the image of a $25\mu\text{m}$ slit used for calibration. In MDR measurements, the droplet is doped with a fluorescent dye and the fluorescence spectrum is measured in a direction perpendicular to the incident light. The light inside the microcavity undergoes total internal reflection and allows only certain modes to propagate in the cavity, depending on the morphology of the cavity. The mode separation in the fluorescence spectrum [16] gives the accurate size of the droplets. The experimental setup consists of a droplet jet that is injected into a vacuum chamber, pumped by a 2000 l/s turbo molecular pump and augmented by cryopumping to maintain pressures as low as 10^{-5} Torr with the droplet jet. We focus the 100fs laser pulses using a 30 cm planoconvex lens and achieve intensities of 10^{15} W cm^{-2} . Experiments with solids are carried on an optically flat plastic by focusing p-polarized light pulses with a 20 cm lens to intensities upto 10^{15} W cm^{-2} , incident at 45° to the normal of the target. We used the plastic target since the atomic composition is not too different from that in the methanol droplets. The target is scanned such that

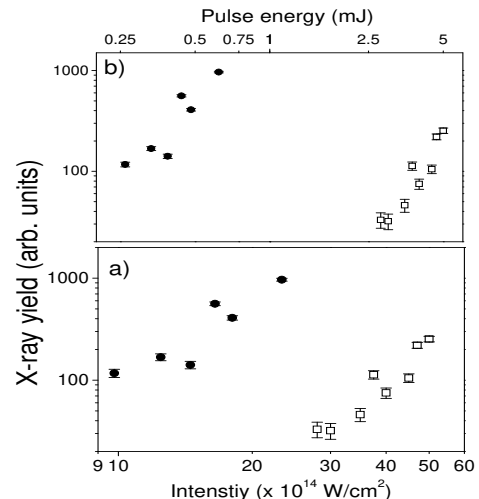


FIG. 2: X-ray emission yields measured for $15\mu\text{m}$ methanol liquid droplet targets (circles) and solid plastic target (open squares) as a function of the incident intensities and pulse energies. The droplets being smaller than the $30\mu\text{m}$ focal spot, only 11% of the incident power interacts with the laser. The data is averaged for the same number of laser shots and corrected for the solid angle of detection.

the each laser pulse is incident at a fresh portion of the target [17]. The x-ray detection in both the experiments were with a NaI(Tl) detector appropriately time gated with the laser pulse, and calibrated using standard radioactive sources.

The x-ray emission spectrum obtained from $15\mu\text{m}$ methanol droplets is shown figure 1 (a). The solid line shows an exponential fit to the data assuming a Maxwellian distribution for the electrons in the plasma. In this fitting we only considered energies larger than 50 keV so that corrections due to the transmission through the glass or aluminum housing of the detector are negligible. To avoid pile up, the count rate was kept less than one per pulse by restricting the solid angle of detection. The X-ray emission spectrum for solid target is shown in figure 1(b) at three times larger intensity, as there was no measurable X-ray emission below $2\times 10^{15}\text{ W cm}^{-2}$. Exponential fit to the data shows that the hot electron temperature is about 31 keV while it is 36 keV in the case of liquid droplets at three times less intensity.

A comparison between the relative integrated X-ray yields from both droplet plasma and plastic target are shown in figure 2(a). Though the intensity ranges used in the microdroplet experiments are different from those used with the solid target we can make a comparison of the yields at an intensity of $2.8\times 10^{15}\text{ W cm}^{-2}$. At this intensity the yield is larger with liquid droplet plasma by more than 250 times. Experiments with higher intensities are not possible with our present laser, since we

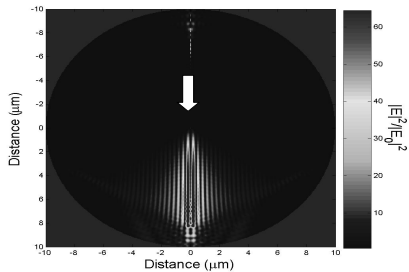


FIG. 3: Computed ratio of the internal to external absolute square electric field inside the droplet cavity calculated for a plane wave incident on a droplet using the Lorentz-Mie theory.

are constrained to maintain a focal spot size of $30 \mu\text{m}$ to ensure that the droplet is close to the center of the focus, despite the spatial jitter of a few microns in the jet. From the measured size of the focal spot we find that the droplets are exposed to only 11% of the incident power. Figure 2(b) shows the x-ray yield as a function of the incident energy that is interacting with the liquid droplets and the solid target. It is very clear that x-ray emission from liquid droplets is very efficient compared to the solid target, even at a fraction of the incident laser power.

At intensities of $10^{15} \text{ W cm}^{-2}$, hot, dense plasmas with hot electrons of about 30 keV temperature are formed mainly by collision-less mechanisms like resonance absorption and vacuum heating etc [18]. A $15 \mu\text{m}$ droplet can not be simply treated as a solid with spherical surface where resonance absorption can take place. On the droplet surface the angle of incidence would vary from 0° to 90° and accordingly the polarization would change from s to p, as we go from the center to the poles of the drop. If we integrate over the incident angle we find that the fractional absorption due to resonance absorption is a factor of 3 less than that for a solid target incident with p-polarization at 45° . A microdroplet is a spherical cavity that scatters light very differently compared to a plain solid. The field that penetrates inside the droplet cavity and that scattered from the spherical surface are different compared to light scattered from a plane-solid target and it is in this scattering that we look for the differences that arises in coupling of the laser energy to plasma in the two cases.

A microdroplet can focus the light entering into the

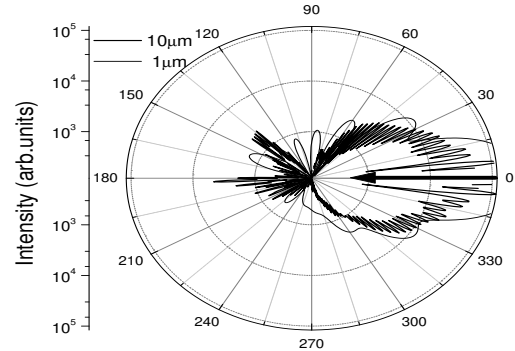


FIG. 4: Angular plot of the intensity of light scattered from the spherical drop. The light is incident along the 0° and is traversing towards 180° . The thick line is scattered diagram for the $15 \mu\text{m}$ drop and thin line is for the $1 \mu\text{m}$ drop.

drop. It is known well known that the spherical cavity can retain the incident energy with a Q factor as large as 10^6 . The incident intensity is expected to be enhanced in and around the droplet surface by two orders of magnitude or more [19]. Lorentz-Mie solutions give a good description of the field propagating in a spherical droplet, at least within the linear approximation, and we use this to numerically calculate the field distribution for a plane wave incident on the droplet [20, 21]. The focal spot size, which is larger than the droplet size enables us to use the plane wave formalism. Figure 3 shows the calculated relative enhancement in the intensity distribution inside the liquid droplet with respect to the incident intensity. The figure shows bright focused spots along both the forward and backward directions. The focusing of the light into small regions in the droplet results from constructive interference of the field propagating in the cavity. Focusing of light inside the cavity is a sensitive function of the size of the cavity and the wavelength of the incident light. Our calculation shows, an increase in intensity by about 60 times close to the surface of the droplet.

It has been shown recently that such focusing of the light and enhancement in intensity in the droplets leads to critical density plasma 'hot spots' of nano-dimension that lead to emission of white light from focused regions at intensities as low as $10^{12} \text{ W cm}^{-2}$ [19]. Calculations in ref.[19] show that at an intensity of $10^{14} \text{ W cm}^{-2}$, the focusing effect leads to energy densities as large as $3 \times 10^3 \text{ J cm}^{-3}$ and upto 95% of the incident energy is absorbed and efficiently coupled into the plasma. It was also shown that at intensities higher than $10^{12} \text{ W cm}^{-2}$

[19], the nano-dimensional hot spots with critical density increase in number and spread in and around the surface of the drop. Light at 10^{12} W cm $^{-2}$ in a solid would not have the same energy density and would not result in critical density plasma. Enhanced energy density in the focused spots leads to plasma with critical density even when the incident energy reaches 10^{12} W cm $^{-2}$, and the energy that follows in the remaining part of the pulse heats the electrons in the plasma hot spots. This effect is somewhat akin to the effective coupling of the laser energy using a pre-pulse that comes ahead of the main laser pulse [22]. So, in addition to the plasma sheath formed on the surface the 'hot spots' contribute to additional absorption of the laser energy and enhancement of the hot electron temperature. It is possible that in addition to the collisional inverse bremsstrahlung mechanisms, collisionless mechanism like resonance absorption at the enhanced intensity takes place in these regions in or about the surface of the drop and contribute to even more effective heating of the electrons.

The light scattered from the surface of a spherical droplet is rippled and non-uniform, in contrast to the interaction with the plane-solid where the field can be assumed to be uniform or a Gaussian along the solid surface. Fig.4 shows that the Lorentz- Mie calculations of the scattered field about the surface. The field scattered along the incident direction (0°) and along the traversing axis (180°) is much larger compared to the direction perpendicular to it. The non-uniformity of field along the surface of the drop has been shown to contribute very effectively to vacuum heating on the surface of the drop. Donnelly *et al* [12] have shown by the PIC simulations for a $1\mu\text{m}$ spherical drop that the non-uniform field surface leads to effective coupling of the laser energy with electrons oscillating not only along the direction of plasma expansion but also along the perpendicular direction, in contrast to the vacuum heating scenario at a vacuum- plane solid interface. They concluded that this effect leads to efficient coupling of the laser energy into a droplet plasma. Fig.4 also shows the scattered electric field for the $1\mu\text{m}$ droplet for comparison. As can be seen from the figure, non-uniformity of the field on the surface could only be larger for droplets of $15\mu\text{m}$ used here and so it is possible that the vacuum heating is more effective in the droplet plasma than in the case of plasma formed on plane solid surface. It is known that rippled surfaces lead to larger fraction of hot electrons and higher X-ray yields, compared to the plane solid surfaces [18]. In principle the non-uniform field rather than a non-uniform surface can have similar effect in giving higher x-ray yields.

In these simple calculations, we do not take into account the changes in refractive index when the plasma is generated and the corresponding changes in light propagation. The analysis requires that for low intensities used in these experiments, substantial pulse energy enters into the cavity before a critical density layer is formed

on the droplet surface. This assumption seems reasonable in view of the recent experiments and calculations [19]. The hot regions inside the droplet can form a high density plasma and absorbs the laser energy efficiently by resonance absorption, producing hot electrons. It is, however, not feasible to compute quantitative contribution of resonance absorption from these plasma regions as the definition of polarization is arbitrary for the small regions and the incident angle is difficult to determine owing to multiple reflections from the droplet surface.

In summary, we have studied x-ray emission from intense laser irradiation of $15\mu\text{m}$ methanol droplets in comparison with that from solids. Our results show that the yields are larger by more than two orders of magnitude with droplet plasmas. Even with 11% of energy incident on the droplet, efficient x-ray generation is produced even at intensities 1.9×10^{15} W cm $^{-2}$. The enhanced efficiency is understood to be due to differences in scattering of the laser light in and about the spherical cavity. The droplet acts like a lens, focuses the light increasing the intensity and the energy density. This leads to efficient coupling of the laser energy to give large x-ray emission yields. Calculations of the scattered field from the surface indicate that the field on the surface would be highly rippled and non-uniform. Taking support of the PIC simulations in Ref. [12] we infer that the vacuum heating contribution can be also much larger in the case of droplet than it would be for solid surface, resulting in a larger fraction of hotter electrons and higher x-ray yields. Finally, these observations have the potential to improve and devise new strategies for development of efficient table-top, pulsed, hard X-ray sources at very moderate intensities that are achievable with much desired high repetition rates of the order of KHz.

-
- [1] R.F.Service, *Science* **301** 154 (2003).
 - [2] B.A.Remington *et.al.* *Science* **284** 1488 (1999).
 - [3] T. Ditmire *et al.*, *Nature (London)* **398**, 489 (1999).
 - [4] T.Cowan *et.al.* *Phys. Rev. Lett.* **84** 903 (2000).
 - [5] S. Fritztler *et al.*, *App. Phys. Lett.* **83**,3039 (2003).
 - [6] M. Schnurer *et al.*, *Phys. Rev. Lett.* **80**, 3236 (1998).
 - [7] P. P. Rajeev, *et.al* *Phys. Rev. Lett.* **90**, 115002 (2003).
 - [8] G.Kulcsar *et.al* *Phys. Rev. Lett.* **84**, 5149 (2000).
 - [9] V. P. Krainov and M. B. Smirnov, *Phys. Rep.* **370**, 237 (2002).
 - [10] L.Rymell and H.M. Hertz *et.al* *Opt. Comm.* **103**, 105 (1993).
 - [11] R. Constantinescu, *et al.*, *Proc. SPIE* **4146**, 101 (2000).
 - [12] T. Donnelly,*et al.*, *J. Phys. B*, **34**, L313 (2001).
 - [13] E. Parra, *et al.*, *App. Phys. A* **77**, 317-323 (2003)
 - [14] H. C. Wu, W. Yu *et. al.*, *App. Phys. B* **77** , 687, (2003).
 - [15] Mc Pherson. A, Thompson B D, *et al.*, *Nature* **370**, 631(1994).
 - [16] M.Anand *et al.*, *Chem. Phys. Lett.* **372** 263 (2003).
 - [17] A.S.Sandhu *et al.*, *Phys. Rev. Lett.* **89**, 225002 (2002).
 - [18] P. P. Rajeev *et. al.*, *Phys. Rev. A* **65** , 052903, (2002).

- [19] C. Favre *et al.*, Phys. Rev. Lett. **89**, 35002 (2002).
- [20] C.F. Bohren and D.R. Huffman, *Absorption and scattering of light by small particles*, John Wiley & Sons, Canada (1983).
- [21] C. Matzler, Matlab functions for Mie scattering and Absorption, (published on the web: www.iapmw.unibe.ch/publications/pdffiles/201.pdf)
- [22] S. Bastiani *et al.*, Phys. Rev. E **56**,7179 (1997).